THE JOURNAL OF INVESTIGATIVE DERMATOLOGY, 65:16–38, 1975
Copyright © 1975 by The Williams & Wilkins Co.
Vol. 65, No. 1
Printed in U.S.A.

THE FINE STRUCTURE OF DEVELOPING HUMAN EPIDERMIS: LIGHT, SCANNING, AND TRANSMISSION ELECTRON MICROSCOPY OF THE PERIDERM

KAREN A. HOLBROOK, PH.D., AND GEORGE F. ODLAND, M.D.

Department of Biological Structure and Department of Medicine, Division of Dermatology, University of Washington, School of Medicine, Seattle, Washington

Eight stages in the development of the human embryonic and fetal periderm have been established, primarily on the basis of surface morphology, major changes in epidermal stratification, and differentiation. The changes in the periderm observed with the scanning electron microscope have been correlated with and supplemented by cytologic studies with the transmission electron microscope in the periderm and other epidermal layers. Light microscopy was used to determine what proportion of the epidermal thickness is accounted for by the periderm and what relationship individual periderm cells have with underlying cells. The results yield a comprehensive, three-dimensional image of the human epidermis during development and support a concept of the periderm as a layer of "dynamic" cells which project superficial blebs, expand in surface area, then regress at the onset of keratinization, leaving only cellular remnants associated with the adult type epidermis.

The developing epidermis of human embryos and fetuses has received a significant amount of attention from early investigators using the light microscope [1–4] and, more recently, from other workers [5–16] who have been concerned with the ultrastructural detail of this tissue. Both types of microscopic studies have yielded considerable data correlating epidermal stratification, cytology, and state of keratinization with different ages of gestation. However, these studies have provided a less satisfactory understanding of the uppermost epidermal layer, the periderm, during development. The periderm first appears as a layer of simple squames, undergoes a series of changes which alter both the surface morphology and the subcellular organization, and then disappears when epidermal keratinization is complete. To comprehend more fully the structural complexity of the periderm, one must study it with methods which yield information of three-dimensional quality.

To date, there has been no adequate or complete study of the surface morphology of the periderm during its entire cycle of development. The intent of this investigation was, therefore, to study a large number of specimens representing many embryonic and fetal ages, to outline a complete sequence of morphologic changes in human periderm, and to present the results by showing the periderm in relation to the full-thickness epidermis. Thus the stage of periderm development could be correlated with the state of differentiation of the underlying epidermal layers. In this systematic analysis, the scanning electron microscope was used to view large areas of the epidermal surface with high resolution at relatively low magnifications. Gross morphology was thus coupled with ultrastructural detail. These observations, correlated with and supplemented by observations obtained by light microscopy and transmission electron microscopy, provided a comprehensive picture of the changes in the surface and subcellular morphology of the periderm.

MATERIALS AND METHODS

Sixty human embryos and fetuses were obtained by hysterectomy, hysterotomy, or saline suction abortion. All embryonic material was received through the courtesy of Dr. Thomas Shepard, Director of the Central Laboratory for Human Embryology. Collecting practices conformed to current recommendations of NIH. In addition, consent forms and collecting practices were approved by the University of Washington Human Experimental Biomedical Review Committee.

Estimated gestation ages (EGA = fertilization age) of the specimens ranged from 36 to 185 days. These ages were determined both from patient histories and fetal measurements. Crown-rump and/or fetal foot lengths were compared against a chart of Shepard [17] to provide the EGA. Samples of skin from the trunk and foot of each specimen were flooded with fixative [18] and cut into large segments for scanning electron microscopy (SEM) and small pieces for light microscopy (LM) and transmission electron microscopy (TEM). All specimens were fixed for 2 hr at room temperature, washed in 0.1 M cacodylate buffer, and postfixed for an additional 1 hr in 1% osmium tetroxide in s-collidine buffer at room temperature. The tissue was then dehydrated through a graded series of alcohols into 100% ETOH. The small

This work was supported by the following grants: USPHS Grants GM 16598, AM 05250, and AM 08368, all from the National Institutes of Health, and by DEO 2600.

Reprint requests to: Dr. K. A. Holbrook, Department of Biological Structure SM-20, University of Washington, School of Medicine, Seattle, Washington 98195.

pieces of skin were placed into propylene oxide and embedded in Epon 812 [19]. The larger segments were removed from 100% ETOH, put into solutions of ETOH-Freon TF (2:1, 1:1, and 1:2) for 15 to 20 min and finally into 100% Freon-TF for 15 to 30 min depending upon the size of the sample. These specimens were then transferred to the pressure chamber of a Bomar SPC-50 critical point bomb, flushed with Freon 13, and taken through the critical point for drying [20].

Critical point dried specimens of skin were affixed, with the periderm oriented upward, to aluminum stubs with silver conducting paint, mounted on a rotary stage in a vacuum evaporator, coated with evaporated carbon and gold-palladium alloy, and viewed in the ETECH Autoscan SEM operated at 20 kv in the secondary electron mode.

Thick and thin specimens of all Epon-embedded skin samples were cut with a Reichert OM U2 or Dupont-Sorvall MT2 ultramicrotome. Thick sections were stained by the method of Huber et al [21] and were photographed at 16× magnification with a Polaroid 545 Land film holder and Polaroid type 55 P/N film. Thin sections were double stained with uranyl acetate (20–30 min) and lead citrate (10 to 15 min) [22] and were observed with the Philips EM 201 TEM. Line drawings (See Figs. 2, 6, 9, 13, 16, 19, 21, 25) illustrating the state of embryonic or fetal development were modified from Patten [23].

RESULTS

Eight stages of periderm development were established on the basis of SEM observations of cell surface morphology. In general, each stage was found to be representative of a 20- to 30-day period of gestation (Fig. 1). It was apparent, however, from inspecting large areas of the surface that there was some variation in the rate of progression of individual periderm cells, even among adjacent cells, through these stages. Thus, in any one specimen, cells characteristic of more than one stage might be encountered.

Stage 1 (< 36 Days EGA—Indifferent Epithelium)

The epidermis of even the youngest embryos (36 days EGA) obtained for this study had already differentiated beyond the single-layered epithelium of stage 1 (Fig. 1). The stage was therefore included in the sequence only as a hypothetical starting point of periderm development.

Stage 2 (36 to 55 Days EGA—Flattened Surface)

Periderm cells characteristic of 35- to 55-day embryos (EGA) (Fig. 2) were seen with the SEM as flat, polygonal cells that were nonuniform in size (9–14 μ diameter). They were modified at the surface by variable densities of microvilli. Only those cells which had a paucity of microvilli showed clearly outlined margins.

Low cuboidal cells of the periderm were seen in thin-sectioned and thick-sectioned specimens (Figs. 3, 4). These cells were united with one another at the surface by junctional complexes and were joined along the remainder of the cell borders by widely separated desmosomes. Cells of both periderm and basal layers had similar cytoplasmic organization. All cellular organelles, including the nucleus, were confined within a peripheral band or central envelope of microfilaments (described as tonofilaments or prototonofilaments). Large masses of glycogen filled in between the filamentous networks. Observations of the cell surface at high magnifications revealed numerous coated vesicles that were open to the amniotic cavity. In both layers of the epidermis, mitotic figures were frequently noted (Figs. 3, 4). At 36 days EGA, a cell which was interpreted as a melanocyte was observed among the cells of the basal layer.

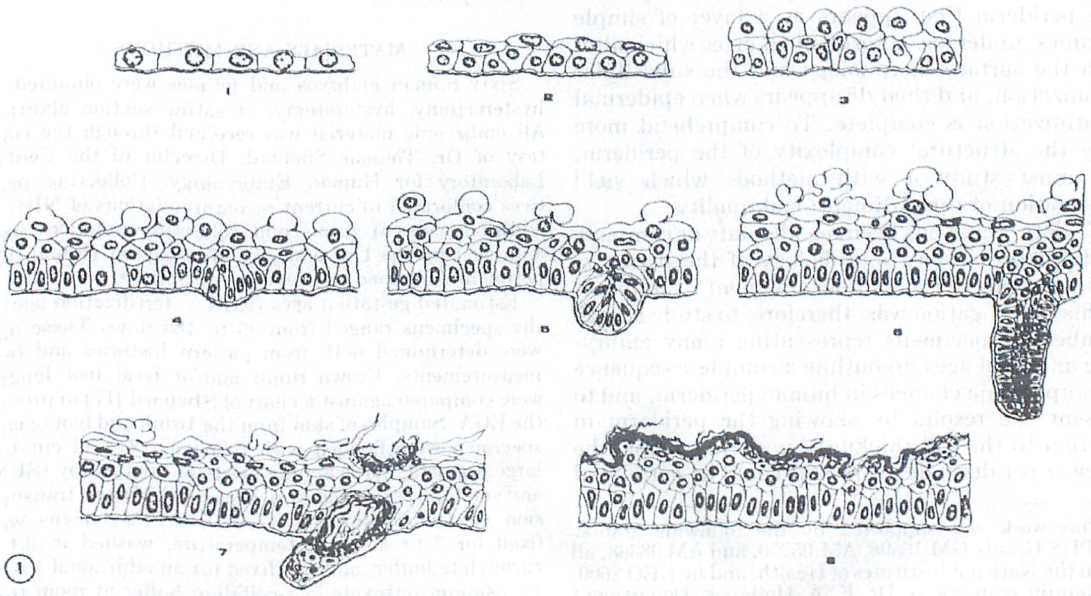

FIG. 1. Schematic diagram of the 8 stages of periderm development and epidermal differentiation. Corresponding estimated gestation ages for each stage are: (*1*) < 36 days, (2) 35–55 days, (*3*) 55–75 days, (*4*) 65–95 days, (*5*) 85–110 days, (*6*) 95–120 days, (*7*) 110–160 days, (*8*) > 160 days.

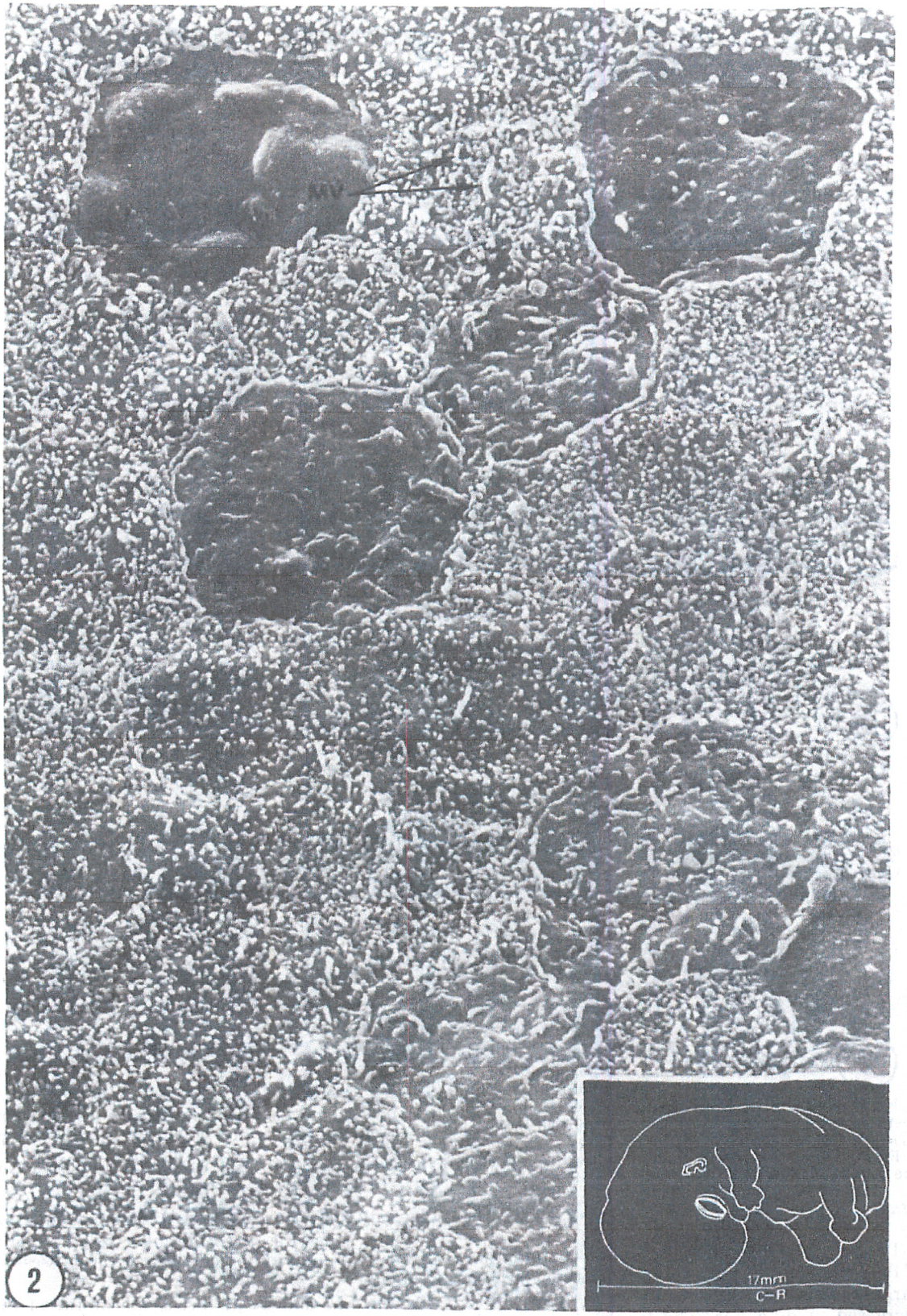

FIG. 2. SEM of 40-day EGA human embryonic skin. Note the variation in cell size and the microvilli (*MV*) (× 4000). *Inset:* Line drawing of a 46-day embryo.

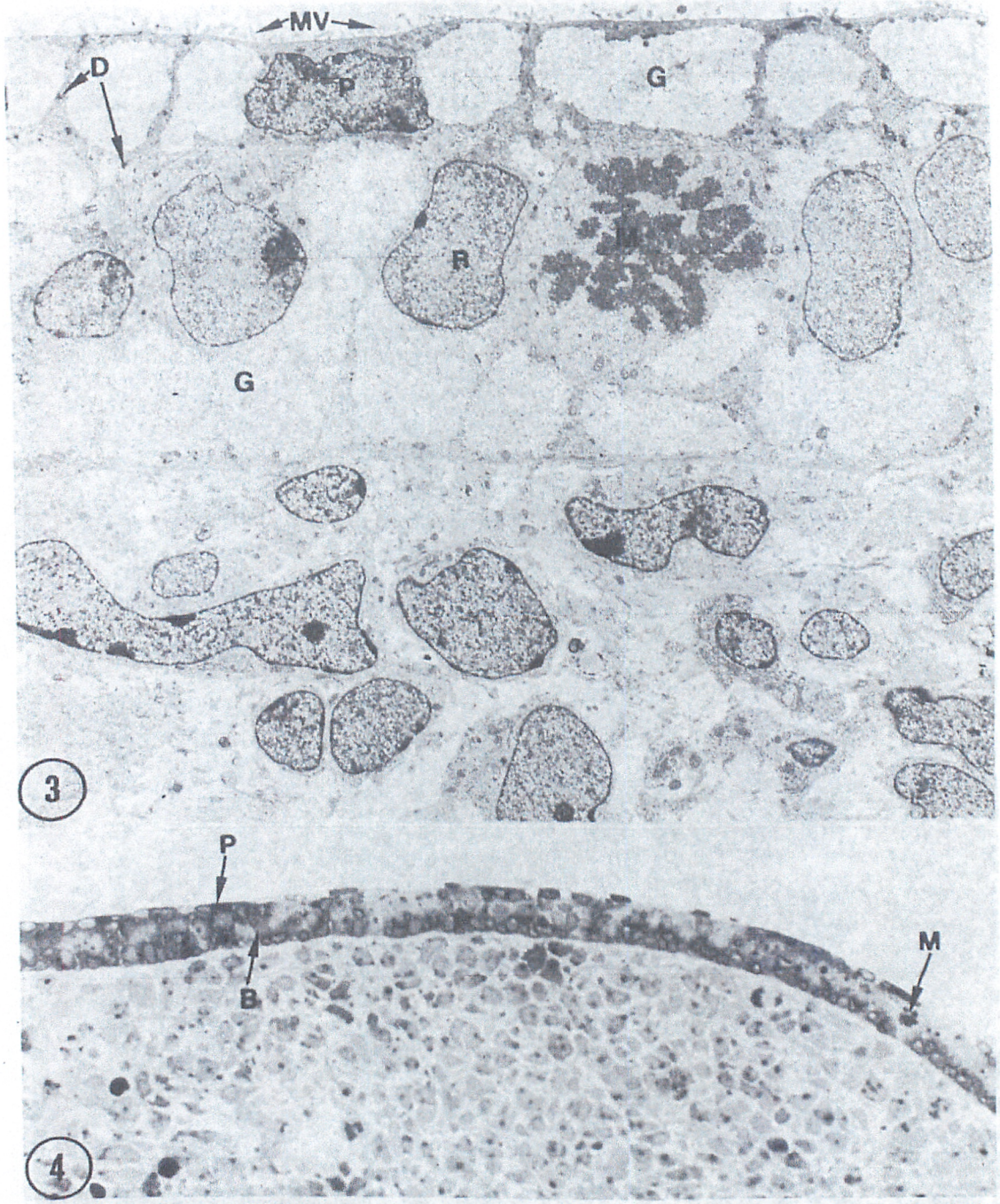

FIG. 3. TEM of 40-day EGA human embryonic skin. Periderm cells (*P*) have a microvillous border (*MV*) and desmosome junctions (*D*). Note the mitotic cell (*M*) within the basal layer (*B*). Cells of both layers contain glycogen (*G*) (× 3450).

FIG. 4. LM of 46-day EGA human embryonic skin. Cells of the periderm (*P*) and basal (*B*) layers are indicated. Note the mitotic cell (*M*) (× 135).

Stage 3 (55 to 75 Days EGA—Elevated Surface)

The periderm layer at stage 3 was a combination of flat and dome-like cells (Fig. 5). Although these varied in size (14–32 μ), all were significantly increased in diameter. The larger of these cells appeared flat and similar to cells of stage 2; the smaller cells were elevated. Toward the end of this stage, all periderm cells showed conspicuous central elevations (Fig. 6). Prominent ridges clearly outlined the individual cells which still possessed microvilli.

At the LM and TEM levels, the profile of the periderm had a scalloped appearance (Figs. 7, 8). Most of the cells had changed from thin pavement epithelial cells to rounded, large-volume cells that

were uniformly covered with microvilli. At high magnifications a thick extraneous "fuzz" coat was observed at the surface of microvilli. Cells of the periderm and intermediate layers still contained abundant glycogen that was compartmentalized within spaces isolated by the now wider marginal and central zones of microfilaments. Less glycogen was noted among cells of the basal layer. There were greater numbers of desmosomes among cells of all layers except between adjacent basal cells. Cells, which appeared to be melanocytes, were observed with greater frequency within the basal layer than in specimens from the previous stage (Fig. 7).

At each stage, the relative size of one periderm cell in a single plane of section was compared against the number of subjacent intermediate cells and indirectly against the number of underlying basal cells. The proportion of the epidermal thickness accounted for by periderm was also estimated from sectioned material. The large diameter and volume of the periderm cells at stage 3 were apparent in thick-sectioned specimens (Fig. 8). Each cell in profile corresponded to 2 intermediate cells and 2 basal cells, and the layer as a whole formed approximately half of the thickness of the entire, now 3-layered, epidermis.

Stage 4 (65 to 96 Days EGA—Incipient Bleb Formation)

Stage 4 appeared to be a period of transition from an epithelium of flat or elevated cells to one characterized by single, rounded blebs. In any one area of skin, cells representing all phases of this transition were noted (Fig. 9). Boundaries of individual cells were more clearly seen where blebs were not yet formed. Nevertheless, cells of all types were measured and found to have an average diameter of 20 μ. As in the previous stage, the amniotic surface of the entire cell retained a microvillous coat.

All stages in the transition of superficial cell morphology were readily apparent in thin-sectioned material studied with the TEM. Elevated, large-volume cells and cells with completely formed single blebs were adjacent to one another in the same section. All showed the microvillous border (Fig. 10) and extraneous coat. The thick and dense subsurface network of microfilaments enclosed mitochondria, dilated cisternae of rough endoplasmic reticulum, the Golgi, and seemingly empty membrane-bounded vesicles. These organelles were also disposed about the nucleus enclosed within a similar and contiguous filamentous meshwork. Glycogen still appeared to account for a significant portion of the cell volume. The cytologic detail of intermediate cells was essentially as described for cells of the periderm (Fig. 10). Clusters of crowded basal cells indicated sites of hair germ formation.

As in the previous stage, the periderm accounted for approximately half of the epidermal thickness and maintained the same 1:2 cell ratio in a single plane of section with underlying intermediate and basal cells (Fig. 11).

Stage 5 (85 to 110 Days EGA—Single Bleb Formation)

All periderm cells were modified at the surface by a large, single bleb (Figs. 12, 13) that obscured most of the cell margin. Blebs of this stage were either globular (Fig. 12) or crenated (Fig. 13) and maintained the same microvillous surface as the remaining basal portion of the cell.

Both the globular and crenated blebs observed with the SEM were seen in thin-sectioned specimens with the TEM. These were attached to the cell by a broad base or a narrow pedicle. Although the SEM gave no indication of different types of periderm cells, studies of thin sections from specimens 100 days EGA showed "light" and "dark" cells (Fig. 14) within this layer.* Both cell types had approximately the same number and type of organelles, microvilli, and extraneous coat and, on the basis of such morphologic criteria, both appeared to be viable. The difference in density between the two cells was accounted for by the organization of microfilaments and glycogen. In the dark cells, a thick peripheral layer of microfilaments containing smooth membrane vesicles and other cell organelles encapsulated a single chamber of glycogen within each bleb (Fig. 14). The light cell, on the contrary, had a more diffuse organization of microfilaments and more widely dispersed glycogen. Microfilaments, interspersed with glycogen, were also the dominant structures within the basal portion of both types of cells. It was within the latter region that the nucleus was most commonly located. Mitotic figures were still seen in the periderm of specimens from stage 5 but not in any later stages. Contacts between adjacent periderm cells as well as periderm-intermediate cell junctions appeared to be strongly reinforced along their contact sites by closely spaced desmosomes (Fig. 14). Glycogen was still abundant in the intermediate cells but was not conspicuous in the cells of the basal layer. The cytoplasm of the latter cells now showed the cytology of a "mature" basal cell.

The epidermis at stage 5 comprised the periderm, two layers of intermediate cells, and the basal layer (Figs. 14, 15). The periderm now accounted for only about one-third the full thickness. Individual periderm cells were 20 to 30 μ in diameter, and by comparisons made from sectioned material, were found to lie directly over 2 or 3 underlying intermediate cells and indirectly above 3 or 4 basal cells. Cords of cells of the developing hair follicles in the hair peg stage extended into the dermis where they were sur-

* The terminology of light and dark cells of the fetal epidermis was previously applied to keratinized and nonkeratinized cells that were seen from replica preparations with the LM [8]; the light and dark cells described here are not equivalent.

rounded by mesenchymal cells of the developing hair bulb (Fig. 15).

Stage 6 (95 to 120 Days EGA—Complex Bleb Formation)

At stage 6, each periderm cell showed clusters of simple and complex blebs projecting from the surface (Fig. 16). All intergrades of bleb formation were seen on the surface of each cell. The smaller blebs were globular; the larger blebs had surface dimpling and complicated infoldings. Scanning electron microscopy also revealed that the blebs were covered with an array of short, dense microvilli and bulbous, smooth membrane protuberances of variable size and morphology (Fig. 16). Frequently these microvilli were morphologically dissimilar from those that modified the surface of the remaining portion of the cell. We concluded from observations of many specimens in the age range of stage 6 that the morphology of microvilli is a highly variable feature (See Fig. 28*a–c*). Outlines of individual periderm cells were easily traced ridges, and measured cell diameters were found to be as great as 60 μ.

The indentations, clefts, and infoldings seen with the SEM were correlated with the intricate channels and compartments seen with the TEM and LM (Figs. 17, 18). The subdivisions of the complex blebs were found to correspond with individual chambers of glycogen, each a separate compartment isolated from others by microfilamentous walls (Fig. 17). Although the periderm was, in many regions, a double layer and consisted of nonhomogeneous cell types, a few characteristics were common to all periderm cells. These included the complex blebs and an increased subsurface density along the plasma membrane. Some of the variation in periderm cell morphology appeared to depend upon the nature of the underlying intermediate cells. Certain cells of the latter layer appeared to contain more dense accumulations of tonofilaments than others and above such cells the nuclei of both light and dark periderm cells were shrunken and greatly indented (Fig. 17). Dark and light cells of the type seen in stage 5 were also seen in specimens of stage 6 (Fig. 17). However, a second type of light cell was also observed in which the cytoplasm was filled with pale diffuse microfilaments and lacked typical cellular organelles.† Desmosomes were still present between these cells and the underlying intermediate layer, but tonofilaments were rarely evident on the periderm side of the membrane at these sites. The uppermost intermediate cells had expanded and flattened in parallel with the cells of the periderm. Both layers of intermediate cells retained a primary composition of glycogen but also showed large accumulations of densely staining tonofilaments located mainly in a peripheral position. Hair follicles extended deep into the dermis and at this stage showed no evidence of keratinization in any part of the structure.

Studies with the LM reinforced the theory of an expanding periderm (Fig. 18). Each periderm cell, in one plane of section, covered 2 to 3 upper-layer intermediate cells but 4 to 5 of the more globular subjacent cells. In profile, one periderm cell corresponded with 6 to 8 basal cells. The periderm still constituted approximately one-third of the epidermal thickness.

Stage 7 (108 to 160 Days EGA—Periderm Regression)

At the midrange of this stage, fetal skin was molded by broad ridges and deep furrows and was well differentiated into follicular and interfollicular regions (Fig. 19). Hair shafts, extending from hair canals, showed the overlapping-scale structure typical of adult hairs. At the base of a hair, keratinized squames were identified (Figs. 19–21) as they lay freely exposed at the skin surface or only partially exposed by loosened edges of overlying periderm cells. All of the interfollicular surface remained covered by flattened and large-diameter (60 μ) periderm cells. Identification of these cells was still based on the presence of blebs and microvilli. At this stage, however, blebs were weakly developed appendages of the periderm. Definition of the blebs was even further diminished in the specimens sampled from fetuses at the end of the age range for this stage (Fig. 20) just before the disappearance of the periderm altogether. At 160 days EGA, smooth-surfaced periderm cells with obscure margins blanketed interfollicular areas. Wax-like bodies (Fig. 21) were observed in the depressions of the surface where keratinized cells were exposed.

Microscopic studies of both thick and thin sections of specimens from stage 7 confirmed that the thin 1-layered or 2-layered periderm constituted a small fraction of the total epidermal thickness (Figs. 22–24). However, the profile of 1 expanded periderm cell now corresponded with the profiles of as many as 10 intermediate cells and 14 basal cells (Fig. 23). At the sites of emergent hairs, periderm cells were peeled away from the surface (Fig. 24). Blebs were seen extending from the surface of the periderm, many of which had a withered appearance and contained a pyknotic nucleus or a nearly unrecognizable "nuclear ghost." At the later stages, in particular, the boundaries that isolated compartments of glycogen appeared to be broken down.

At 140 days EGA, the dark (Figs. 22, 24) and light (Figs. 23, 24) cells were observed. The dark cells had the same cytoplasmic characteristics as the cells from the previous stage of complex blebbing (Fig. 22). They were characterized by a dense border of microfilaments and large, compact masses of glycogen. One additional, previously unreported feature was noted: ribosomes were aligned along the entire periphery of the cell, beneath the plasma membrane and in association

† Such cells were described by Breathnach [15] as "transformed" cells.

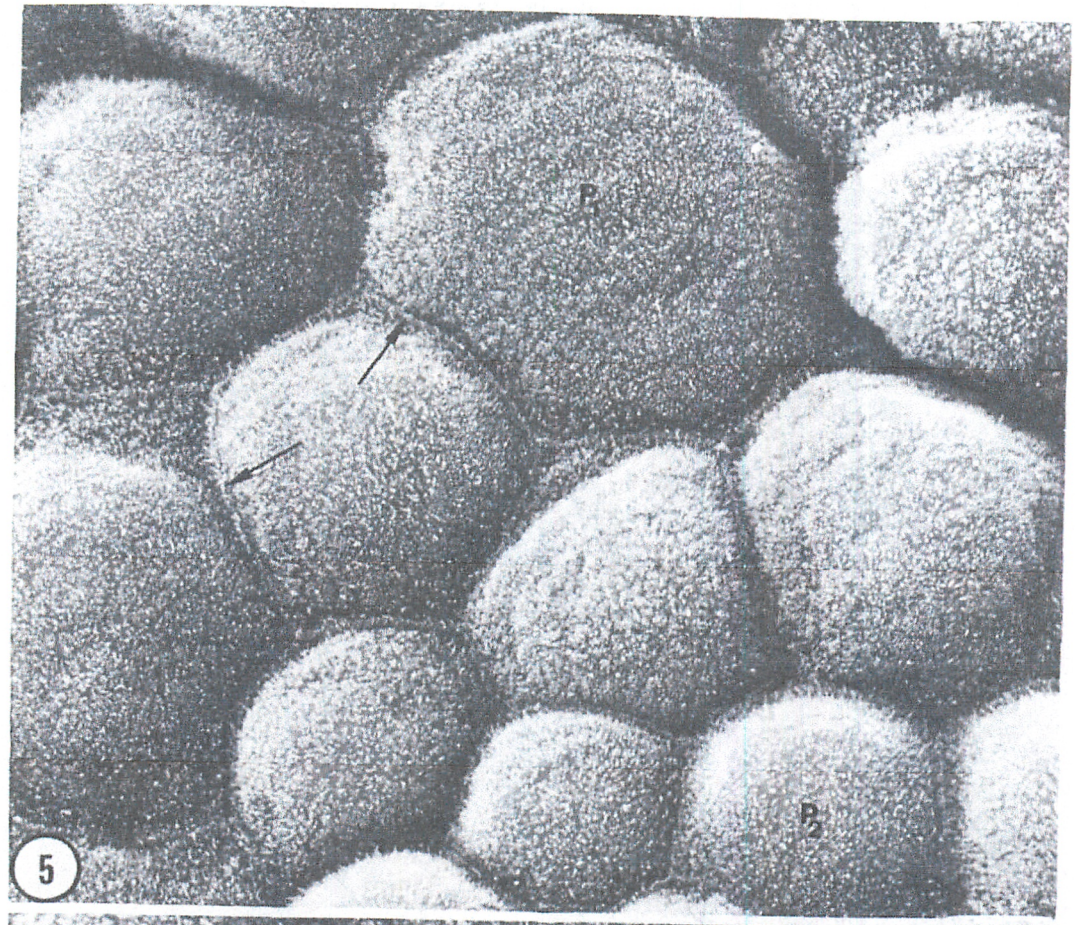

FIG. 5. SEM of 60-day EGA human fetal skin. Flat, large-diameter cells (P_1) and elevated, small-diameter cells (P_2) are both seen in the periderm. Note the conspicuous cell boundaries (*arrows*) (× 2000).

FIG. 6. SEM of 70-day EGA human fetal skin. All periderm cells show a central elevation (*) and prominent cell borders (*arrows*) (× 2660). *Inset:* Line drawing of a 70-day fetus.

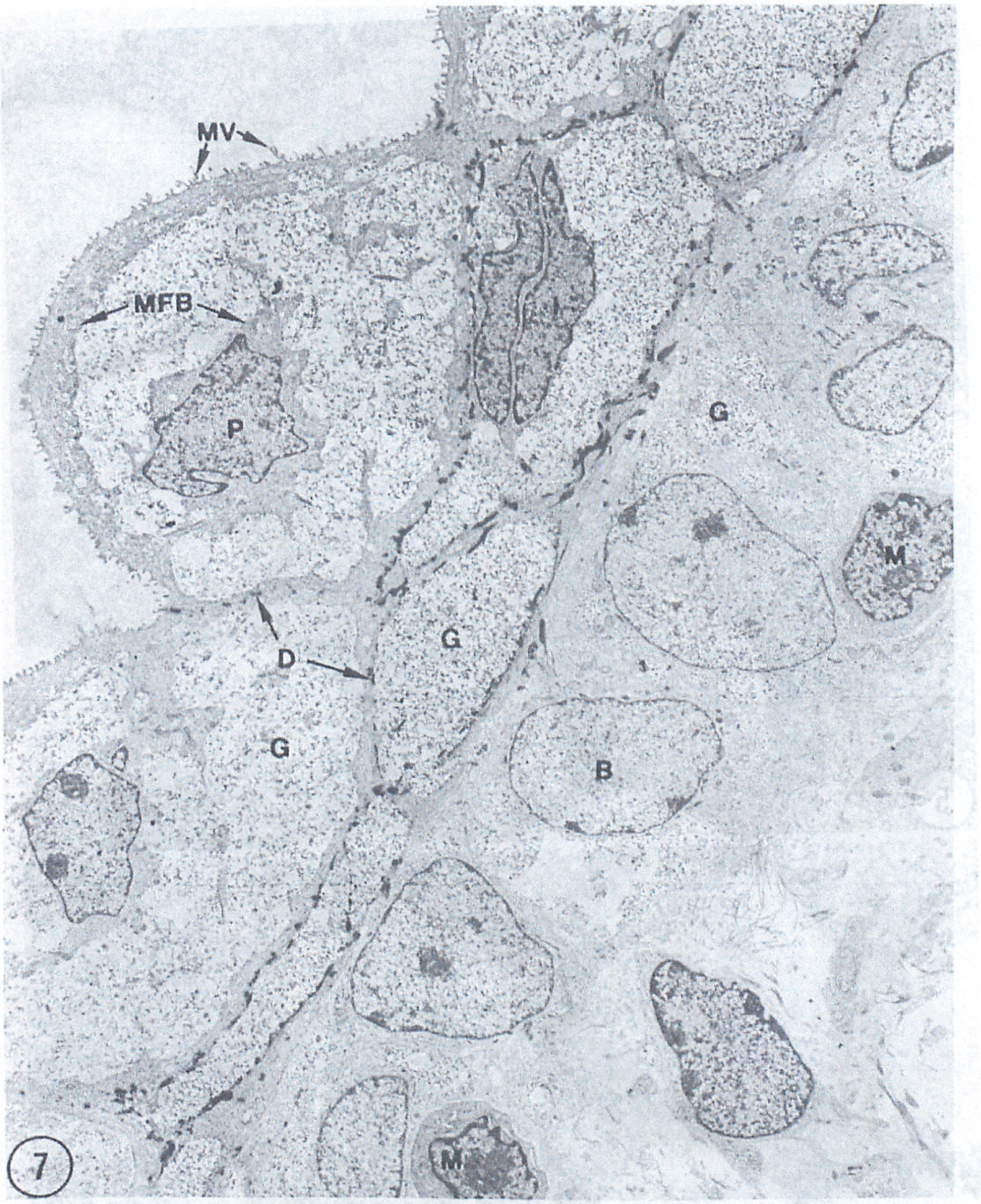

FIG. 7. TEM of 75-day EGA human fetal skin. Large-volume periderm cells (*P*), intermediate cells (*I*), and cells of the basal layer (*B*), including melanocytes (*M*), compose the epidermis. Note the glycogen (*G*) and desmosomes (*D*) of all layers, and the microfilamentous bands (*MFB*) and microvilli (*MV*) of periderm cells (× 3700).

FIG. 8. LM of 75-day EGA fetal skin. Note the large cytoplasmic volume of the periderm cells (*P*), the proportion of the epidermis that is made up of periderm and the ratio of P cells to intermediate (*I*) and basal (*B*) cells (× 80).

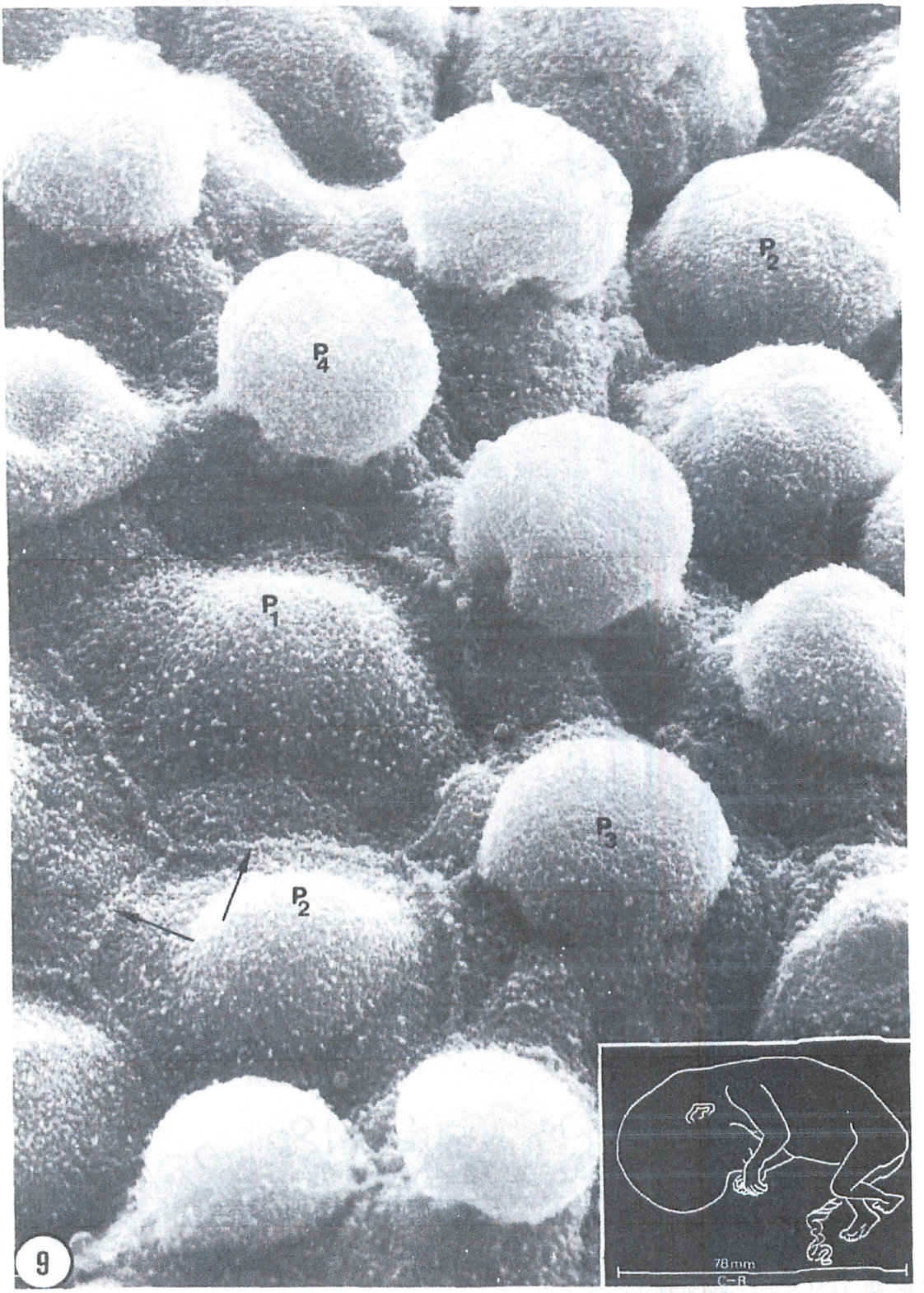

FIG. 9. SEM of fetal skin at 88 days EGA. Note the flat-surfaced cells (P_1), elevated cells (P_2), cells with incompletely formed blebs (P_3), cells with completely formed blebs (P_4), and conspicuous cell borders (*arrows*) (× 2970). *Inset:* Line drawing of an 84-day fetus.

FIG. 10. TEM of fetal skin at 86 days EGA. Elevated periderm cells (P_2) are adjacent to a cell with a completely formed bleb (P_4). Intermediate (*I*) and basal (*B*) layers, glycogen (*G*), microvilli (*MV*) and microfilamentous bands (*MFB*) are apparent (× 2860).

FIG. 11. LM of fetal skin at 80 days EGA. Note the contribution of periderm (*P*) to the total epidermal thickness and the relationship of P cells to intermediate (*I*) and basal (*B*) cells (× 80).

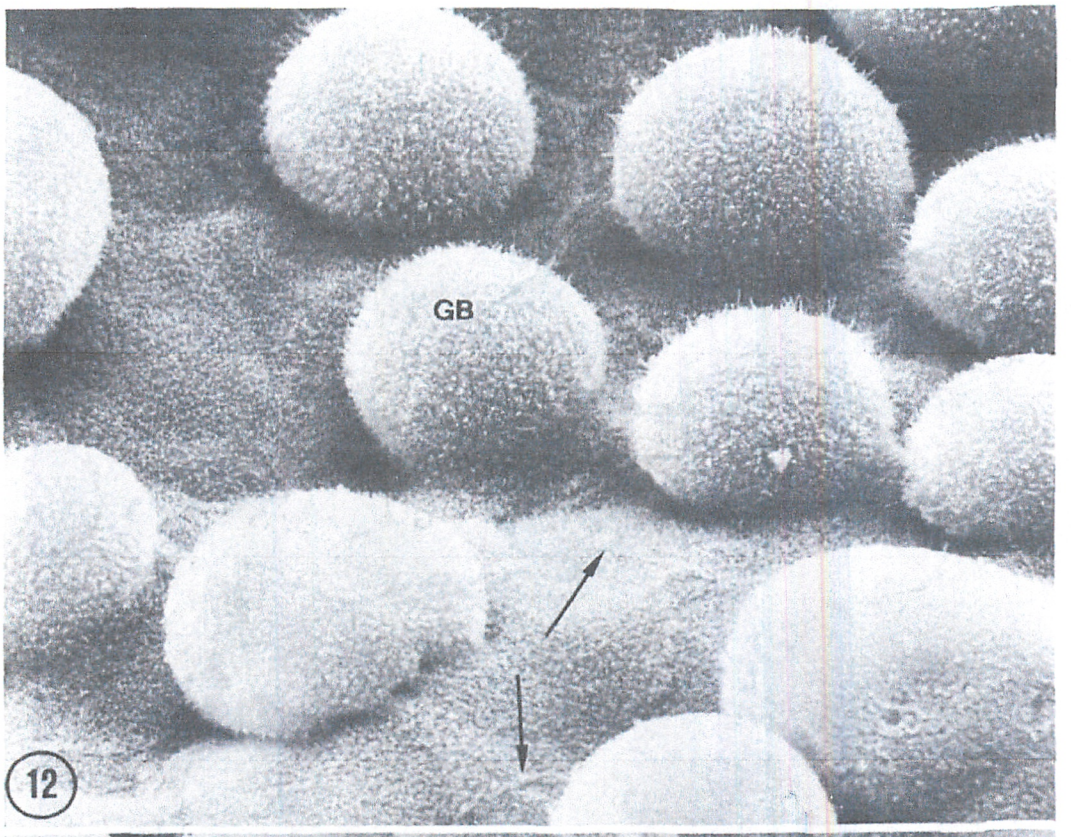

FIG. 12. SEM of fetal skin at 100 days EGA. Single globular blebs (*GB*) project from periderm cells. Cell margins (*arrows*) are evident (× 2500).

FIG. 13. SEM of fetal skin at 100 days EGA. Blebs (*CB*) are crenated and cell margins (*arrows*) relatively obscure (×2500). *Inset:* Line drawing of a 100-day fetus.

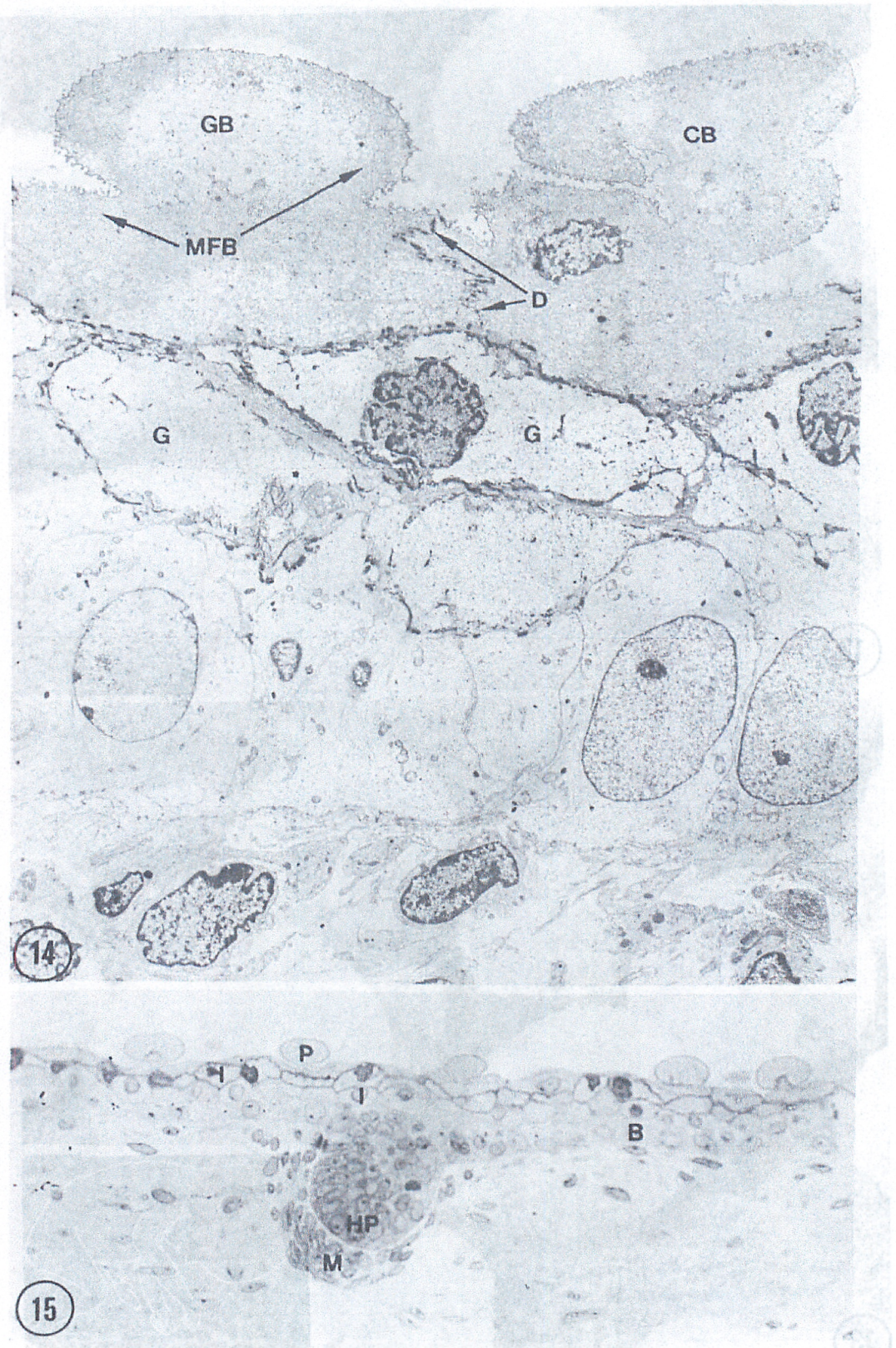

FIG. 14. TEM of fetal skin at 95 days EGA. Globular blebs (*GB*), crenated blebs (*CB*), and microfilamentous bands (*MFB*) containing smooth membrane vesicles and other organelles are evident in cells of the epiderm. Note the glycogen (*G*) and the frequency of desmosomes (*D*) among cells of the periderm and intermediate layers (× 3500).

FIG. 15. LM of fetal skin at 95 days EGA. Note the relationship of one periderm cell (*P*) to underlying intermediate (*I*) and basal (*B*) cells, the hair peg (*HP*) and surrounding mesenchymal cells (*M*) (× 80).

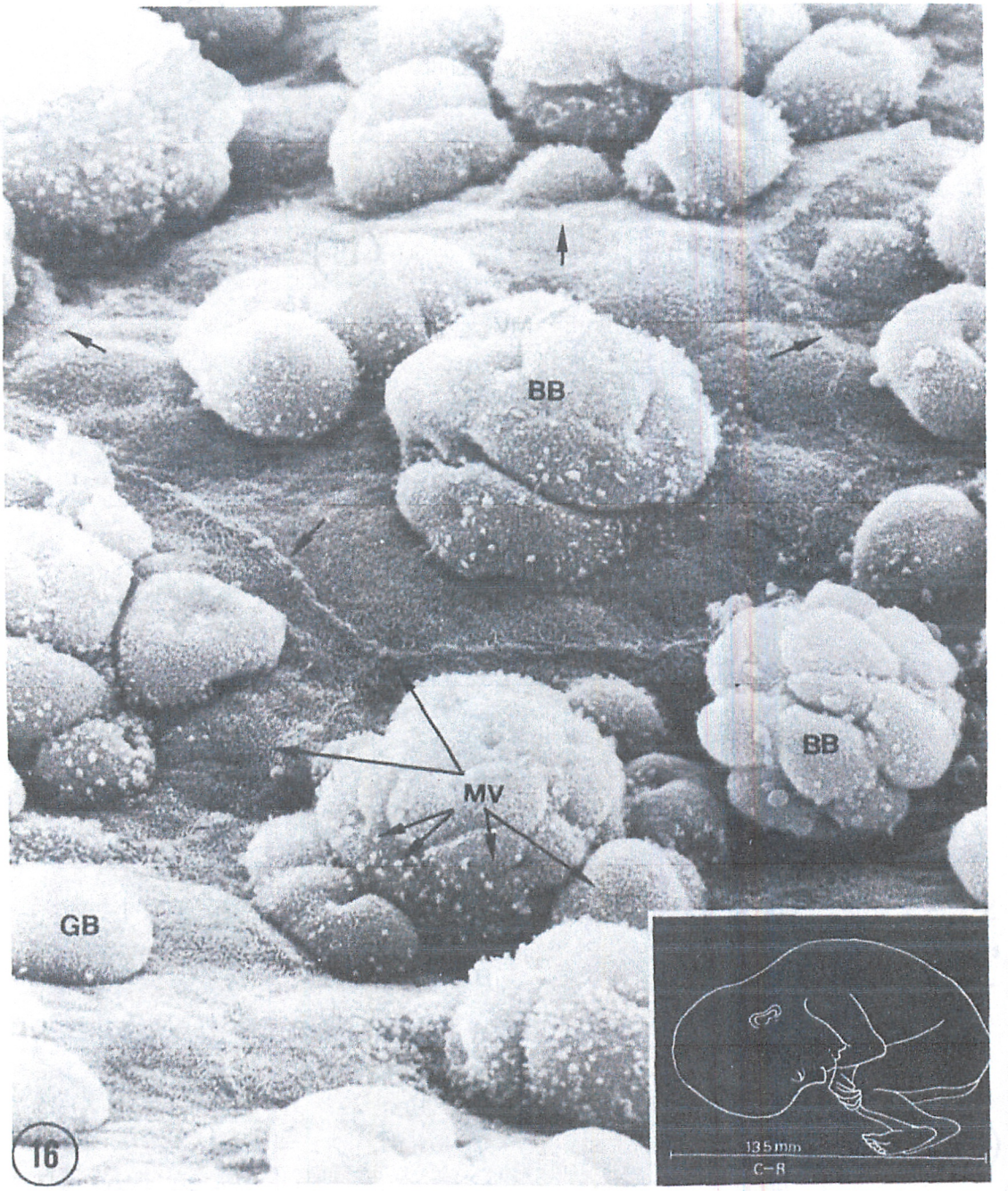

FIG. 16. SEM of fetal skin at 112 days EGA. Complex blebs (berry-like, *BB*), simple blebs (*GB*), and margins (*arrows*) of periderm cells are apparent. Note the expanded area of a single periderm cell and the variation in structure of microvilli (*MV*) (× 2100). *Inset:* Line drawing of a 112-day fetus.

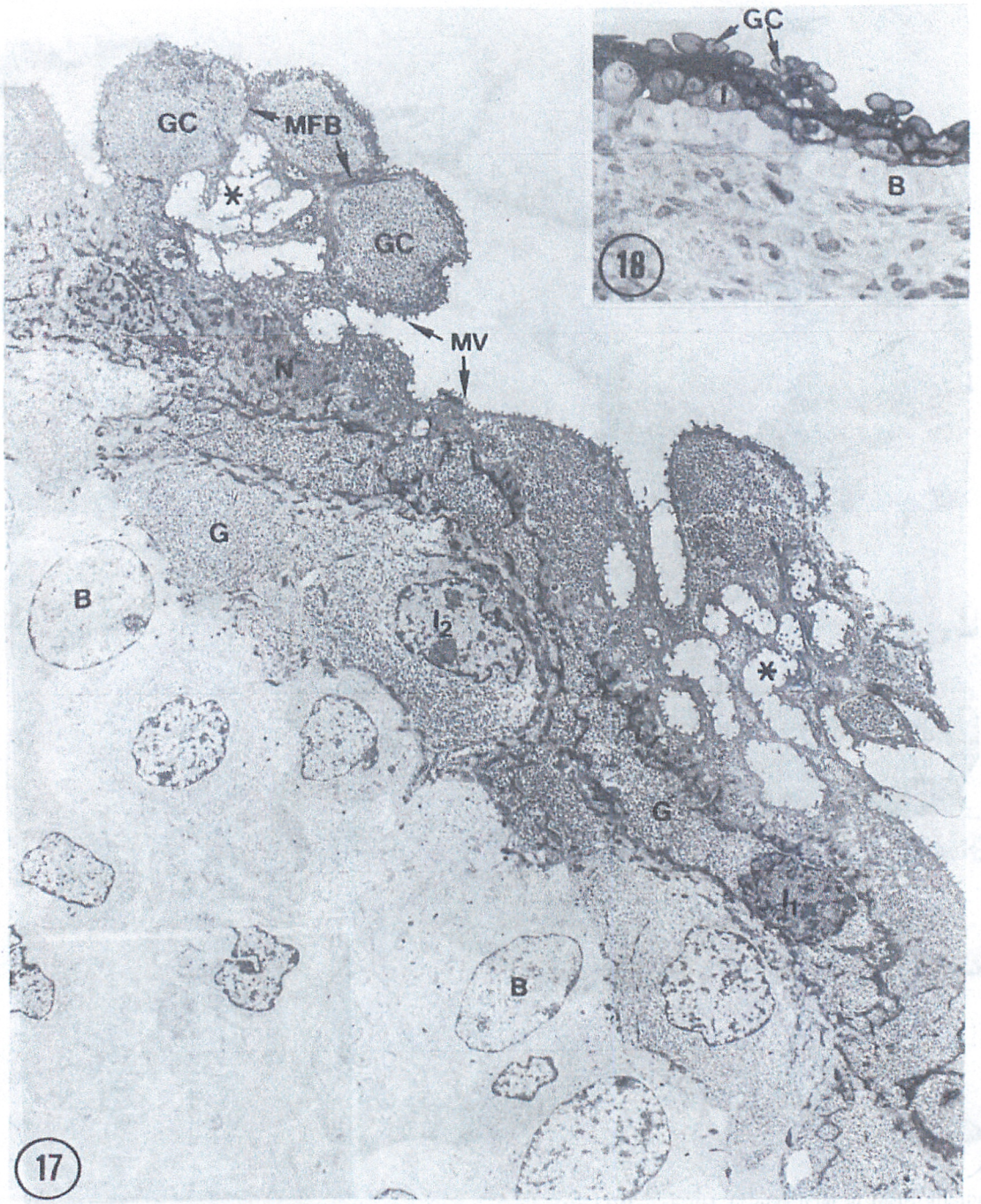

FIG. 17. TEM of fetal skin at 108 days EGA. Note the channels (*), glycogen compartments (*GC*), microfilamentous walls (*MFB*), nucleus (*N*), and microvilli (*MV*) of complex blebs of "dark" periderm cells; glycogen (*G*), cell shape, and tonofilamentous density of the two intermediate cell layers (I_1 and I_2) and the basal cells (*B*) (× 2650).

FIG. 18. LM of fetal skin at 108 days EGA. Complex blebs and glycogen compartments (*GC*) of periderm cells (*P*) are seen superficial to intermediate (*I*) and basal (*B*) cell layers (× 75).

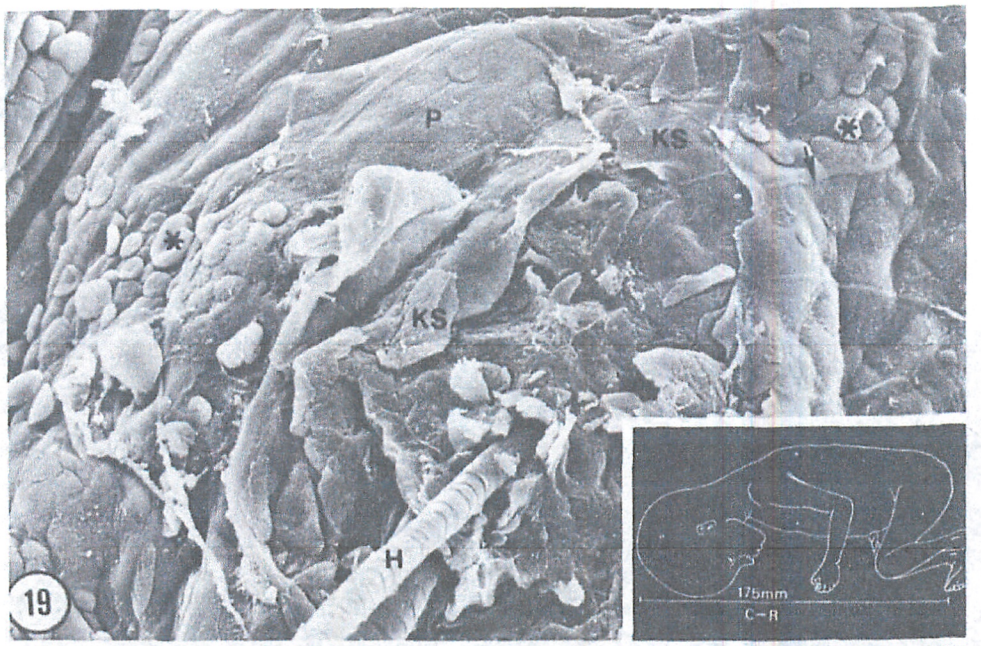

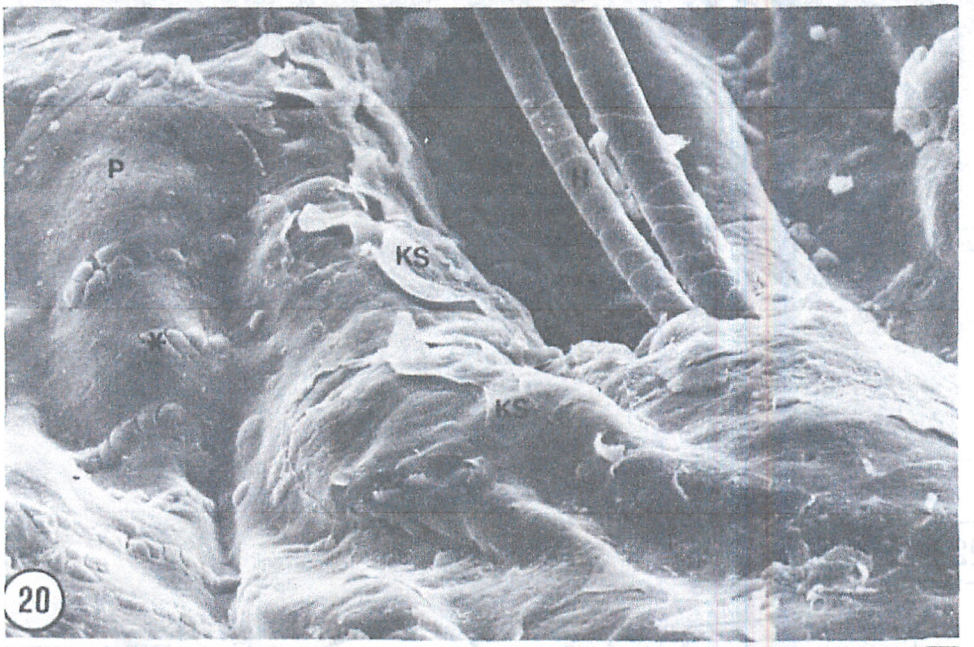

FIG. 19. SEM of fetal skin at 140 days EGA. A hair (*H*) and keratinized squames (*KS*) are seen in the follicular region and large, transformed periderm cells (*P*) with reduced blebs (*) are apparent in the interfollicular region. *Arrows* indicate margins of periderm cells (× 565). *Inset:* Line drawing of a 140-day fetus.

FIG. 20. SEM of keratinized fetal skin at 160 days EGA. Note hairs (*H*), keratinized squames (*KS*), flat periderm cells (*P*) with diminished blebs (*). Boundaries separating adjacent periderm cells are obscure (× 540).

FIG. 21. SEM of keratinized fetal skin, 160 days EGA. Note the surface detail of a keratinized squame (*KS*) and the wax-like body (*WA*) on the skin surface (× 1480). *Inset:* Line drawing of a 160-day human fetus.

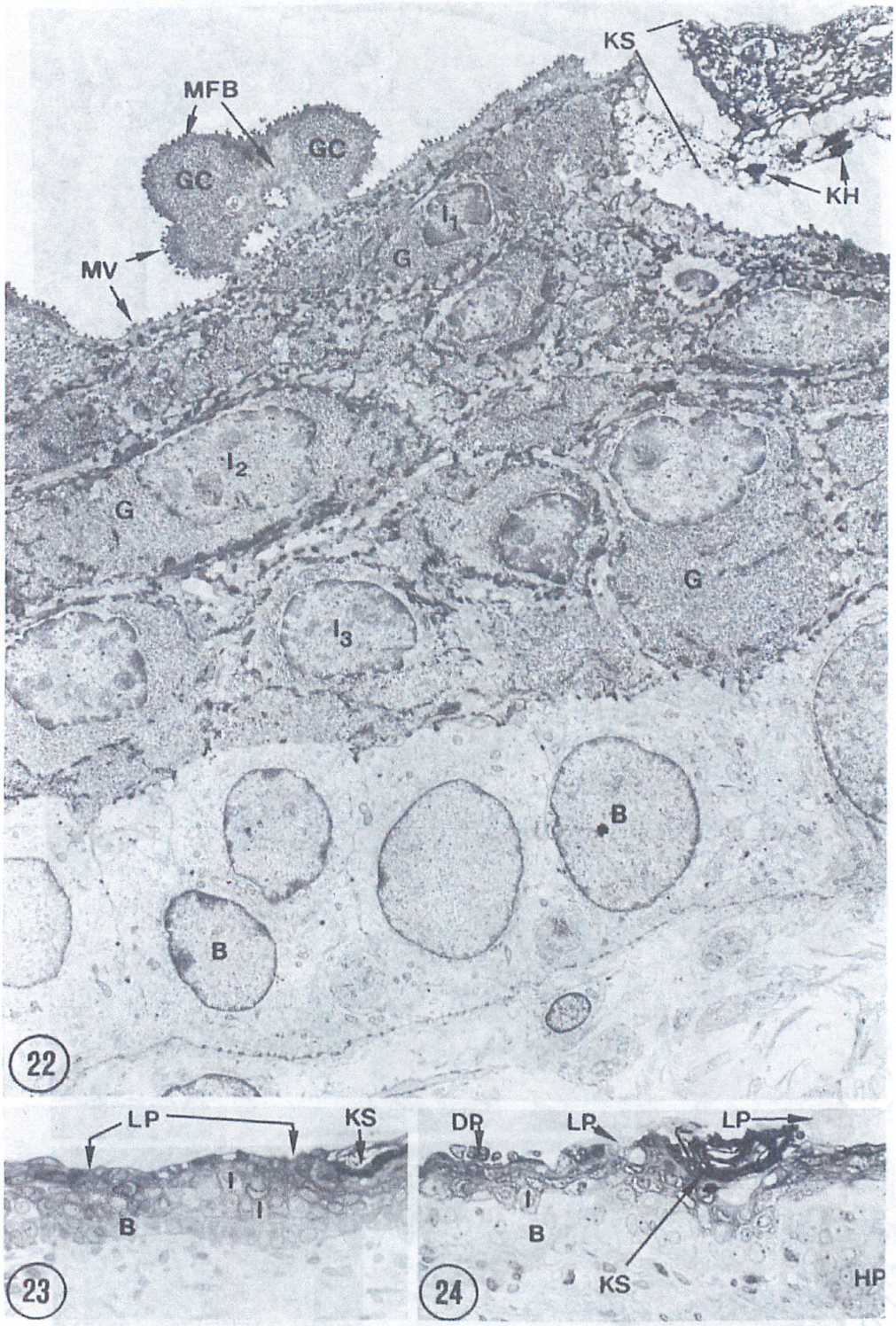

FIG. 22. TEM of fetal skin at 130 days EGA. Portions of several incompletely keratinized cells (*KS*) with keratohyalin (*KH*) are apparent at the site of a hair follicle. Part of one "dark" periderm cell is seen in the interfollicular region. Note the microfilament (*MFB*) isolated glycogen compartments (*GC*) of the periderm bleb and the thin basal portion of the remainder of the cell. Microvilli (*MV*) extend from the surface. Compare the glycogen (*G*) content and density of tonofilaments among cells of the 3 intermediate layers (I_1, I_2, I_3) and the basal layer (*B*) (× 3380).

FIG. 23. LM of 130-day EGA fetal skin. "Light" periderm cells (*LP*) are evident. Note the spread of one periderm cell (*between arrows*), the keratinized cells (*KS*) at the site of an emergent hair, and intermediate (*I*) and basal (*B*) layers (× 72).

FIG. 24. LM of fetal skin at 128 days EGA. "Light" (*LP*) and "dark" (*DP*) periderm cells are apparent. Note the keratinized cells (*KS*) of a hair follicle, cells of the hair peg (*HP*) and intermediate (*I*) and basal (*B*) layers (× 72).

with the thickened submembranous substance. More of the light cells had the pale and finely filamentous substructure with little or no glycogen (Fig. 23). Blebs often showed empty cytoplasmic centers. Partially detached cells of the periderm were always light cells (Fig. 24). None of the intermediate cells in the interfollicular areas was keratinized.

In the last ages of stage 7 (approximately 160 days EGA), the morphology of periderm cells appeared further altered toward that of the light cell. Junctions between the periderm and subjacent cells were either modified or absent. In many instances, fragments of degenerated periderm cells were all that remained of this layer above the keratinized cells of the newly formed stratum corneum. The waxlike bodies observed with the SEM to lie in the skin crevices above the keratinized cells were seen in thin-sectioned specimens as dense, flocculent globules with discrete surface boundaries.‡

The remaining layers of the epidermis now formed a 4-layered to 5-layered epithelium (Figs. 22–24). Intermediate cells still contained glycogen but, in addition, included more tonofibrillar bundles. In the oldest specimens from this stage (160 days EGA), the uppermost cells of this layer showed keratinous changes of thickened membranes, organelle deterioration, and small amounts of keratohyalin. In some instances, a few layers of immature horny cells that contained nuclei were observed.§ Extensive cellular debris was noted between the newly keratinized cells and the periderm remnants. A true granular layer was observed only in association with the hair follicle. At these sites, more fully mature squames were also noted, both at the surface and lining the hair canal. Remnants of fiber-filled cells and other debris accumulated about the hair within the canal.

Stage 8 (160 Days EGA—Cornification)

Stage 8 more accurately describes a stage of epidermal differentiation than peridermal development, for it was at this stage that no remnants of the periderm remained and the epidermis had characteristics of the adult type tissue. Smooth-surfaced polygonal cells were seen in the SEM in both follicular and interfollicular areas (Fig. 25). These cells measured significantly less in diameter (20–30 μ) than the periderm cells which formed the surface of the epidermis at stage 7. Cell boundaries were also less distinct and surface features less remarkable; blebs and microvilli were absent.

Studies with both the LM and TEM confirmed the absence of a periderm layer or periderm remnants over any of the surface of the skin (Figs. 26, 27). The fetal epidermis at 185 days EGA was completely keratinized and consisted of a basal layer, 2 or 3 spinous layers of cells still containing variable amounts of glycogen, a true granular layer with distinct keratohyalin, and 5 or 6 layers of stratum corneum (Figs. 26, 27).

DISCUSSION

Stages of the Periderm Cycle

The development of the periderm and underlying layers of the human embryonic and fetal epidermis in the first 6 months of intrauterine life was studied by means of LM, TEM, and SEM. The results were reported in a series of 8 stages (Fig. 1), which were separated on the basis of periderm surface morphology, subcellular cytology, cell diameter and volume, relationship with underlying epidermal cells and stratification, and differentiation of cells in the remaining epidermal layers.

For the most part, other workers who have studied periderm development have either described features of a periderm cycle in general or presented the ultrastructural details of periderm cells at one of a few stages within the cycle. The latter aspect, the TEM data of periderm development (Figs. 3, 7, 10, 14, 17, 22, 26), was included in this study to supplement the observations from SEM, to tie periderm development to the overall phenomena of epidermal differentiation, and to relate this work to previous ultrastructural investigations of the periderm [4–16]. Our studies were primarily in agreement with other published observations of the periderm except in the timing of specific events. This could be expected on several accounts. First, accurate aging of specimens from patient histories is tenuous. Second, authors have often failed to specify whether they were reporting menstrual age or estimated gestation age of a specimen, and finally, observations of the periderm have been reported without identifying the region of the body from which the sample was taken. It is known that epidermal, hence peridermal, differentiation is dissynchronous in the various regions of the body [1,7,12,15,27]. Unlike these earlier studies, however, it was not our purpose to concentrate on the fine points of periderm ultrastructure at any one age, but rather to develop an overall concept of the periderm during its full cycle of development.

Zastava [1], Wolf [10], and Hoyes [12] were the only investigators to look at the entire sequence of periderm development and to subdivide the events into specific stages. Zastava and Wolf both outlined a series of stages based on changes in the structure of the cell surface. Using a pseudoreplica technique [28] and LM or TEM, these authors observed changes in the periderm surface during

‡ These substances may be secretions of vernix caseosa from the sebaceous gland or some unknown amniotic debris [12]. The pilosebaceous apparatus was fully developed in these specimens and is known to be functional. Even though newly formed stratum corneum has a coat of vernix caseosa, the composition of that material—sebum, periderm cell remnants, shed lanugo hairs, and closely packed squames [24–26]—would have a more complex ultrastructure than the bodies described in this study.

§ These cells are thought to be representative of a transient phase of incomplete or aberrant keratinization resulting from the transformation of cells with minimal keratohyalin content [15] or without keratohyalin [10].

FIG. 25. SEM of fetal skin at 165 days EGA. Keratinized cells (*KS*) are evident in both interfollicular and follicular regions. Note the emergent hair (*H*) (× 1000). *Inset:* Line drawing of a 170-day fetus.

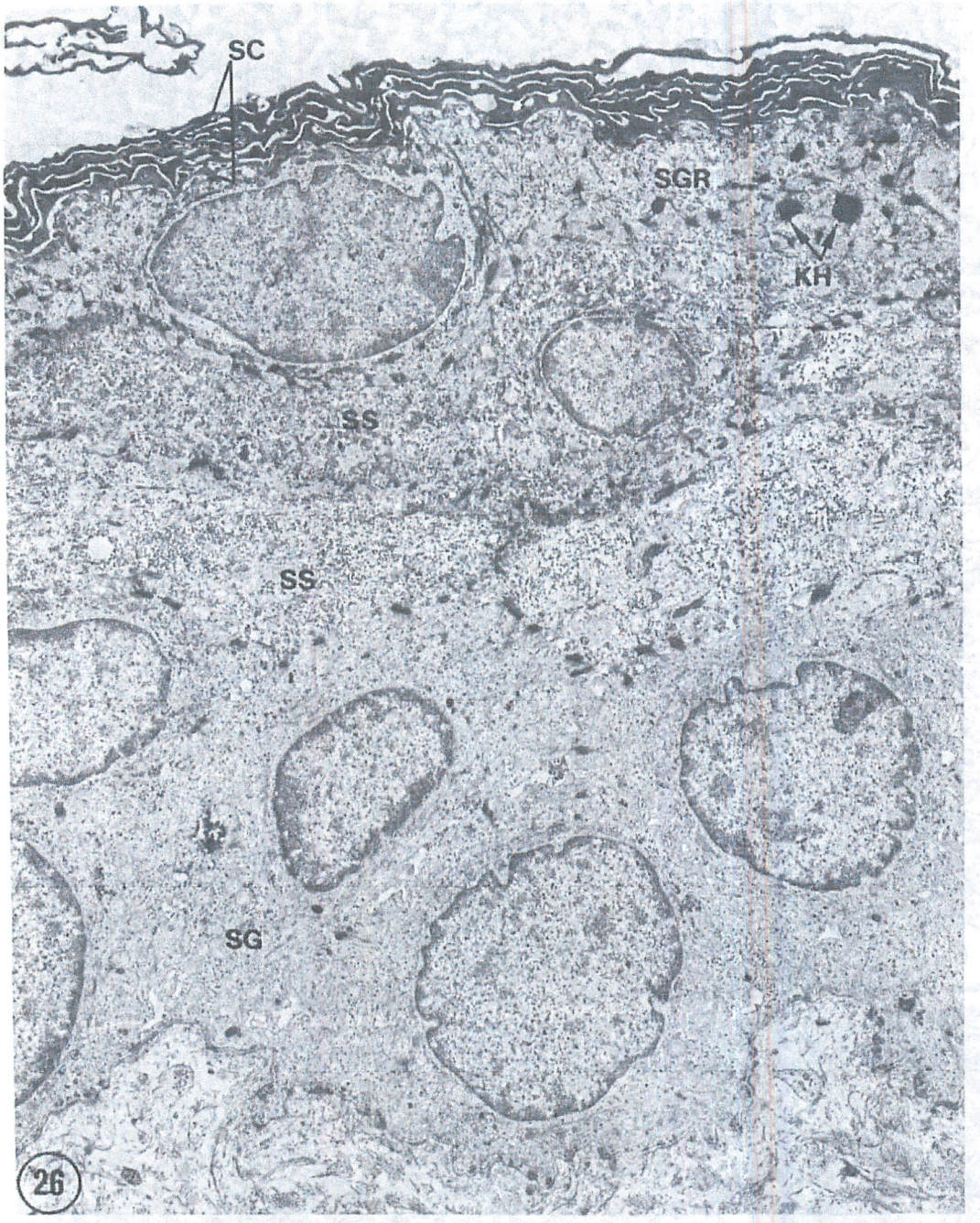

FIG. 26. TEM of fetal skin at 185 days EGA. Layers of stratum corneum (*SC*), stratum granulosum (*SGR*), stratum spinosum (*SS*), and stratum germinativum (*SG*) are evident. Note the presence of keratohyalin (*KH*) and the abundance of glycogen in the SG and SS (× 4950).

FIG. 27. LM of 185-day EGA fetal skin. There is complete keratinization of the skin (*SC*) in the interfollicular region. Note the absence of all periderm cells or remnants (× 115).

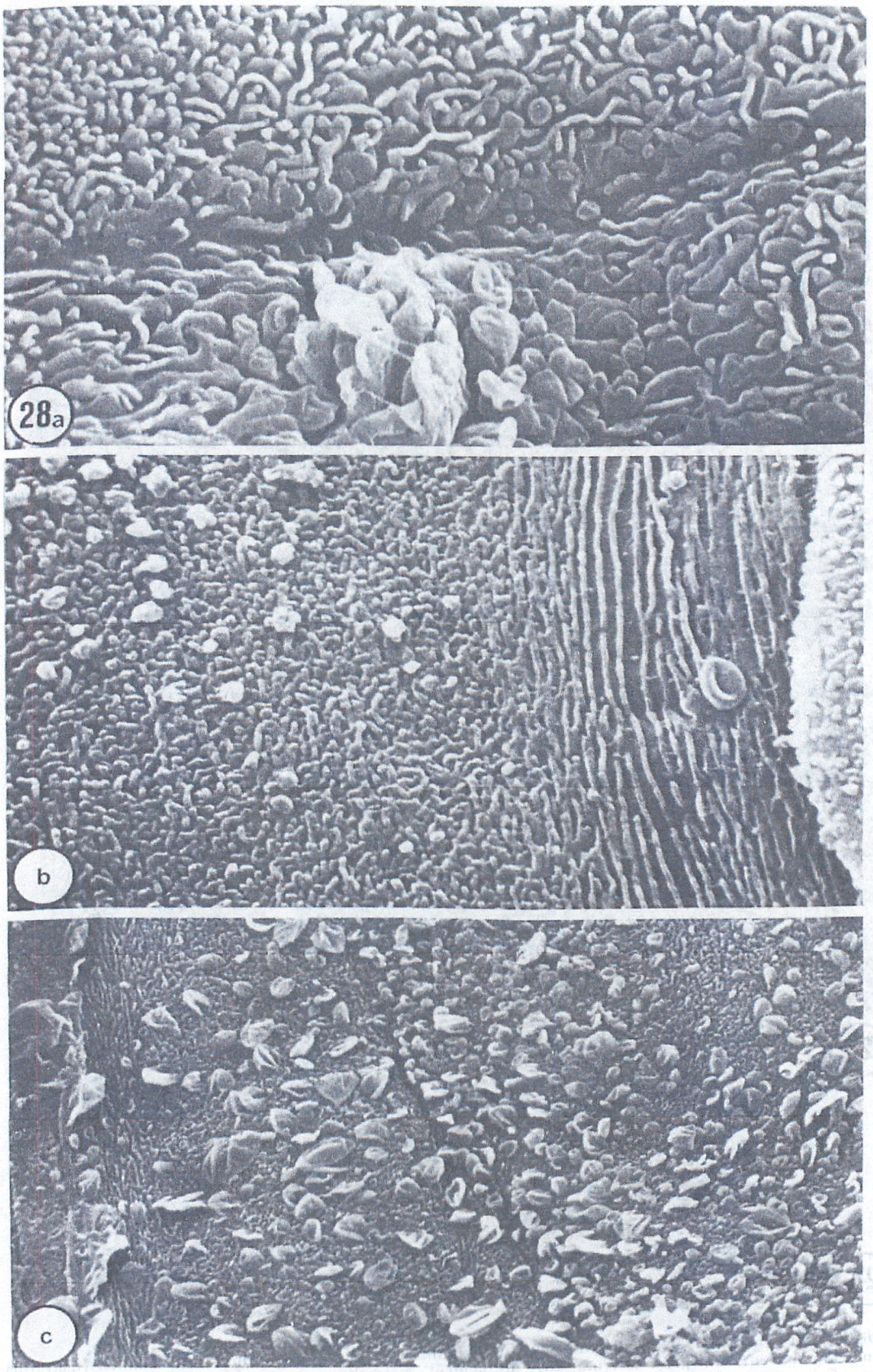

FIG. 28. SEM of microvilli from adjacent cells of 100-day EGA fetal skin. Each micrograph is of one cell and shows the variation in morphology of microvilli (*a*, × 11,000; *b*, × 7630; *c*, × 2600).

development. Although their work provided a new look at the periderm, the information obtained was limited by the resolution of the technique. Hoyes [12] studied the ultrastructure of the periderm at several ages of gestation in order to identify a period of periderm cell function. On the basis of purely morphologic criteria, he divided the periderm cycle into three stages which he believed to be representative of the three phases of periderm function. In our study, the stages were separated not on the basis of function but rather, like those of Zastava and Wolf, on features of the cell surface. However, we have supplemented their general scheme with new information about cell surface structure as seen with the SEM (Figs. 2, 5, 6, 9, 12, 13, 16, 19–21, 25, 28), estimated gestation ages at which the stages occurred, and with ultrastructural detail of both the periderm and other epidermal layers at each stage as observed by TEM.

Potential of the Periderm Cell

In preparing the present scheme of periderm development, we became aware of two questions relating to the potential of an individual periderm cell. First, does each periderm cell itself pass through all the stages of development then die, or does any given periderm cell develop only one set of morphologic characteristics (one stage), then become replaced by another cell with a different set of characteristics? This question is mainly concerned with the rate of periderm cell turnover. From studies of periderm morphology, most authors have implied that one cell type is molded into another by elevation of new and increased numbers of surface blebs which are then pinched from the surface and lost into the amniotic fluid.

If periderm cells are continually replaced, then we would expect to observe mitotic figures in this layer and/or subjacent layers at all stages and we would anticipate finding desquamated periderm cells in the amniotic fluid. Neither appeared to be the case. From our observations of a large number of specimens, mitotic figures were not seen in cells of the periderm any later than 93 days EGA. Breathnach and Robins [13] reported mitotic activity in the periderm to cease between 42 and 126 days, and Hoyes [12] restricted periderm mitoses to the time period he defined as stage 1, early differentiation (56–77 days). By methods of radioautography, Gerstein [29] obtained similar results from a study on epidermal cell proliferation in fetal skin; mitoses in a 126-day specimen were observed only among basal cells. He interpreted this observation as a necessary increase in number of cells in the lower layers to keep pace with the expanding surface area.

Cells that were distinctly peridermal in origin were seen, by TEM studies, in the precipitate collected after centrifugation of amniotic fluid [30]. These "cells" resembled detached simple and complex blebs more than entire, desquamated cells. The only complete cells that have been reported in the many studies of amniotic fluid cytology were regressed cells of the periderm and keratinized squames [24,31,32]. The observation of detached blebs, but not of whole periderm cells from stages before regression, supports the argument that individual periderm cells pass through all stages of development and are not continually replaced at each stage. It is not surprising, however, that whole periderm cells, from a stage of regression, or keratinized cells were noted. Regressed periderm cells peel away from the epidermal surface after keratinization in the underlying layers (Figs. 19, 20, 24), and horny cells are regularly shed with epidermal turnover.

Thus, studies of the morphology and kinetics of the epidermis and amniotic fluid cytology indicate that a single periderm cell can undergo a remarkable series of changes which expand and modify the surfaces into a series of complex and often bizarre morphologies.

The second aspect of periderm cell potential questions the involvement of this cell in the keratinization of the epidermis. Are the periderm cells and the keratinized cells two distinctly different generations of cells, two independent sets of transforming cells, or is there a transition of periderm cells into keratinized cells? Wolf [4] has suggested that the periderm is a keratinized layer subject to destruction in the amniotic fluid, a degenerated keratinized layer, or an "anomalously keratinizing keratinized layer." All morphologic studies support the theory that the specific alterations observed in periderm cells (loss of organelles, membrane thickening, filamentous loading) are not the same changes or, at best, are an incomplete set of changes, which transform the underlying epidermal cells into keratinized squames. Moreover, cells of the periderm have never been observed to contain keratohyalin. Thus, if the changes in the periderm are a form of keratinization, the mechanism must differ from that which forms a definitive stratum corneum [12]. However, we have seen that the periderm and intermediate cells are altered simultaneously; this suggests that either one layer responds to changes in the other or that both layers are independently capable of responding to some stimulus for transition. In this respect, it would be of interest to investigate what, if any, influences the amniotic fluid has on this aspect of epidermal and peridermal transformation.

Function of the Periderm Cell

The periderm may be no more than a protective layer of the epidermis [25] and may function in this capacity before keratinization. However, many features of the periderm cells reported in this work (abundant microvilli, blebs, coated and smooth membrane vesicles, extraneous coat and increasing cell size) and in part by others [14–16], may be interpreted in terms of an active periderm cell function. Most of these characteristics are modifi-

cations of the cell surface associated with an increase in surface area, presumably to subserve secretory and/or absorptive functions. Microvilli covered by an extraneous "fuzz" coat of mucopolysaccharide [33] are characteristic of all periderm cells (Figs. 2, 3, 5–7, 9, 10, 12–14, 16, 17, 19, 22). Microvilli are thought to hold exudates on the cell surface, house uphill pumps for rapid transport of sugars (there is evidence for a role by microvilli in glucose transport), provide a source of membrane for an increase in area when a cell spreads, and to serve as a mechanism to maintain a constant surface as a cell goes through dynamic changes [34]. All of these functions are appropriate to a theory of periderm activity.

Periderm cells may be important in the uptake of glucose from the amniotic fluid. The microvilli and fuzz coat are very similar to the modifications of the intestinal mucosa cell at its luminal border. Others have discussed whether polysaccharides (glycogen) associated with the fetal epidermis are synthesized from carbohydrates extracted from the amniotic fluid [25,35]. In the early fetus, the skin is rich in glycogen (Figs. 3, 7, 10, 14, 17, 22, 26). Although little is known about the appearance and concentration changes of glycogen in this tissue, it has been reported from quantitative studies [36] that glycogen is present in greatest abundance and remains nearly constant when periderm cells have reached a maximum size and are modified by simple and/or complex blebs and microvilli (Figs. 12–18). At this time, the cells are morphologically most indicative of functional activity. The glycogen concentration decreases significantly at approximately stage 6 when thickened membranes of the periderm cells were noted. Thus the time of decrease in cutaneous glycogen corresponds with a period in periderm morphology that signals approaching epidermal keratinization and peridermal regression. The decrease in epidermal glycogen at this stage may reflect an inability of the altered periderm cell membrane to transport glucose; as a consequence, glycogen stores within the cells may be utilized and depleted. The decrease in cutaneous glycogen does not reflect an overall decrease in glycogen from the body; in fact, at this stage other fetal tissues show an increase in glycogen concentration [36].

The small, smooth membrane vesicles located within the marginal layer of microfilaments were most evident at the peak of periderm development (Fig. 14). These have been cited as evidence for pinocytotic uptake of amniotic fluid [14] or secretion of either amniotic fluid or extraneous coat [4, 6,12]. Wolf [4] and Hoyes¶ concluded that the periderm at its peak of development is involved in amniotic fluid production and that after periderm regression, this role is taken over by cells of the umbilical cord or the amnion. Their contention was not supported by experimental evidence.

Direct physiologic data, however, show that the epidermis before keratinization definitely does function in material transport. Parmley and Seeds [37] measured the permeability of human fetal skin to isotopic water at various ages. By correlating these permeability data with both the morphology of fetal skin and the chemical composition of the amniotic fluid, these authors showed that the decrease in permeability is coincident with keratinization and that both occur at about the same time as a significant change in amniotic fluid composition occurs. When the skin is a freely permeable system, the chemical composition of amniotic fluid is comparable to serum dialysate; however, the skin becomes essentially impermeable at a time when amniotic fluid is primarily a product of fetal renal excretion. Although the study of Parmley and Seeds has provided clear evidence that the periderm is capable of transport, the positive identification of the substances transported and the direction in which they move still remain unanswered. When these aspects are documented with experimental evidence, it may then be possible to uncover a role of the periderm and its amniotic fluid environment in epidermal differentiation.

In one of the earliest studies of the human fetal epidermis, Wolf [4] assessed the state of knowledge of the periderm: "The temporary and relatively long-standing presence of the periderm during the development of the covering epithelium of the body surface is one of the most mysterious processes in the development of the skin." (p 296). Although the enigmatic nature of this layer has been, at least somewhat, abated by ultrastructural information that has been revealed over the past 15 years, a total concept of the periderm during development has not been presented. In this regard, the present study has provided a comprehensive view of the human periderm and epidermis from a state of indifferent ectoderm to an adult type stratum corneum with methods of microscopy that revealed both surface (SEM) and subcellular structure (TEM). We believe that these results establish a baseline of morphologic information that can be used for future experimental investigations related to the developing epidermis.

The authors gratefully acknowledge the expert technical assistance of Mrs. Mary Hoff, Mrs. Pamela Joseph, and Mrs. Elizabeth Merrick, and thank Dr. William D. Perkins for critical reading of the manuscript.

REFERENCES

1. Zastava VL: Vesikulosinipovrch peridermu embryonálni kůže člověka. Biologické Listy Suppl 2:215–226, 1950
2. Hale AR: Morphogenesis of volar skin in the human fetus. Am J Anat 91:147–173, 1952
3. Serri F, Montagna W, Huber WM: Studies of skin of the fetus and the child: the distribution of alkaline phosphatase in the skin of the fetus. Arch Dermatol 87:234–245, 1963
4. Wolf J: Structure and function of the periderm. I. Superficial structure of the periderm epithelium. Folia Morphol (Praha) 15:296–305, 1967

¶ Personal communication to Breathnach [14].

5. Bonneville M: The periderm of human fetal skin, Electron Microscopy. 1964 Proceedings of the Third European Regional Conference, Prague, Volume B. Edited by M Tittbach. London, Royal Microscopical Society, 1965, pp 565–566
6. Breathnach AS, Wyllie LM: Fine structure of cells forming the surface layer of the epidermis in human fetuses at fourteen and twelve weeks. J Invest Dermatol 45:179–189, 1965
7. Hashimoto K, Gross BG, Dibella RJ, Lever WF: The ultrastructure of the skin of human embryos. IV. The epidermis. J Invest Dermatol 47:317–335, 1966
8. Wolf J: Structure and function of the periderm. II. Inner structure of periderm cells. Folia Morphol (Praha) 15:306–317, 1967
9. Wolf J: The relation of the periderm to amniotic epithelium. Folia Morphol (Praha) 15:384–392, 1967
10. Wolf, J: The replacement of periderm by epidermis. Folia Morphol (Praha) 16:24–35, 1968
11. Wolf, J: Curve of development and disappearance of peridermal phase of human embryonic skin demonstrated by the replica method. Folia Morphol (Praha) 16:36–42, 1968
12. Hoyes AD: Electron microscopy of the surface layer (periderm) of human fetal skin. J Anat 103:321–336, 1968
13. Breathnach AS, Robins J: Ultrastructural features of epidermis of a 14 mm (6 weeks) human embryo. Br J Dermatol 81:504–516, 1969
14. Breathnach AS: Embryology of human skin. J Invest Dermatol 57:133–143, 1971
15. Breathnach AS: An Atlas of the Ultrastructure of Human Skin. London, Churchill, 1971
16. Whittaker DK, Adams D: The surface layer of human foetal skin and oral mucosa: a study by *scanning and transmission electron microscopy*. J Anat 108:455–464, 1971
17. Shepard TH: Growth and development of the human embryo and fetus, Endocrine and Genetic Diseases of Childhood. Philadelphia, Saunders, 1969, pp 1–6
18. Karnovsky MH: A formaldehyde–glutaraldehyde fixative of high osmolarity for use in electron microscopy (abstr). J Cell Biol 27:137A, 1965
19. Luft JH: Improvements in epoxy resin embedding methods. J Biophys Biochem Cytol 9:409–414, 1961
20. Cohen AL, Marlow DP, Garner GE: A *rapid critical* point method using fluorocarbons ("Freon") as intermediate and transitional fluids. J Microsc (Oxf) 7:331–342, 1968
21. Huber JD, Parker F, Odland GF: A basic fuchsin and *alkalinized methylene blue rapid stain for epoxy*-embedded tissues. Strain Technol 43:83–87, 1968
22. Reynolds ES: The use of lead citrate at high pH as an electron opaque stain in electron microscopy. J Cell Biol 17:208–213, 1963
23. Patten BM: Human Embryology. Third edition. New York, McGraw–Hill, 1968
24. Nieland ML, Parmley TH, Woodruff JD: Ultrastructural observations on amniotic fluid cells. Am J Obstet Gynecol 108:1030–1042, 1970
25. Serri F, Montagna W: The structure and function of the epidermis. Pediatr Clin North Am 8:917–941, 1961
26. Biezenski JJ, Pomerance W, Goodman J: Studies on the origin of amniotic fluid lipids. Am J Obstet Gynecol 102:853–861, 1968
27. Montagna W: The Structure and Function of Skin. Second edition. New York, London, Academic, 1962
28. Wolf J: *Über die Herstellung mikroskopische praeparate der Oberflächen mit Hilfe der Adnaestonsmethode*. Z Wiss Mikrosk 56:181–201, 1939
29. Gerstein W: Cell proliferation in human fetal epidermis. J Invest Dermatol 57:262–265, 1971
30. Hoyes AD: Ultrastructure of the cells of the amniotic fluid. J Obstet Gynaecol Br Commonw 75:164–171, 1968
31. Bishop EH, Corson S: Estimation of fetal maturity by cytologic examination of amniotic fluid. Am J Obstet Gynecol 102:654–664, 1968
32. Votta RA, Bobrow De Gagneten C, Parada O, Guilietti M: Cytological study of amniotic fluid in pregnancy. Am J Obstet Gynecol 102:571–577, 1968
33. Hoyes AD: Acid mucopolysaccharide in human fetal epidermis. J Invest Dermatol 48:598–601, 1967
34. Porter K, Prescott D, Frye J: Changes in surface morphology of Chinese hamster ovary cells during *the cell cycle*. J Cell Biol 57:815–836, 1973
35. Bonsnes RW: Composition of amniotic fluid. Clin Obstet Gynecol 9:440–448, 1966
36. Sharp F: A quantitative study of the glycogen content of human fetal skin in the first trimester. J Obstet Gynaecol Br Commonw 78:981–986, 1971
37. Parmley TH, Seeds AE: Fetal skin permeability to *isotopic water (THO) in early pregnancy*. Am J Obstet Gynecol 108:128–131 1970

This document is a scanned copy of a printed document. No warranty is given about the accuracy of the copy. Users should refer to the original published version of the material.